Molecular Biology of the Cell
Vol. 20, 3390–3400, July 15, 2009

Scribble Interacts with β-Catenin to Localize Synaptic Vesicles to Synapses

Yu Sun,* Mytyl Aiga,* Eileen Yoshida,* Patrick O. Humbert,† and Shernaz X. Bamji*

*Department of Cellular and Physiological Sciences and the Brain Research Centre, University of British Columbia, Vancouver, BC, V6T-1Z3, Canada; and †Cell Cycle and Cancer Genetics Laboratory, Peter MacCallum Cancer Centre, East Melbourne 3002, VIC, Australia

Submitted December 5, 2008; Revised April 8, 2009; Accepted May 12, 2009
Monitoring Editor: Thomas F.J. Martin

An understanding of how synaptic vesicles are recruited to and maintained at presynaptic compartments is required to discern the molecular mechanisms underlying presynaptic assembly and plasticity. We have previously demonstrated that cadherin–β-catenin complexes cluster synaptic vesicles at presynaptic sites. Here we show that scribble interacts with the cadherin–β-catenin complex to coordinate vesicle localization. Scribble and β-catenin are colocalized at synapses and can be coimmunoprecipitated from neuronal lysates, indicating an interaction between scribble and β-catenin at the synapse. Using an RNA interference approach, we demonstrate that scribble is important for the clustering of synaptic vesicles at synapses. Indeed, in scribble knockdown cells, there is a diffuse distribution of synaptic vesicles along the axon, and a deficit in vesicle recycling. Despite this, synapse number and the distribution of the presynaptic active zone protein, bassoon, remain unchanged. These effects largely phenocopy those observed after ablation of *β-catenin*. In addition, we show that loss of β-catenin disrupts scribble localization in primary neurons but that the localization of β-catenin is not dependent on scribble. Our data supports a model by which scribble functions downstream of β-catenin to cluster synaptic vesicles at developing synapses.

INTRODUCTION

Synapse formation begins with the recognition of appropriate targets and formation of incipient contacts and is followed by the recruitment of pre- and postsynaptic proteins to points of cell–cell contact (Ziv and Garner, 2004). The formation of presynaptic active zones, sites of neurotransmitter release, is believed to occur by the insertion of large dense-core vesicles containing multiple active zone components in a preassembled form (Ahmari *et al.,* 2000; Zhai *et al.,* 2001). Similarly, clusters of pleiomorphic vesicles associated with synaptic vesicle (SV) proteins are recruited and localized to regions underlying active zones (Ziv and Garner, 2004). These elements were previously thought to be relatively stable in mature synapses; however, emerging evidence from time-lapse imaging suggests that there is constant movement of SVs and other synaptic proteins into and out of individual synapses (Krueger *et al.,* 2003; Bamji *et al.,* 2006; Kalla *et al.,* 2006; Tsuriel *et al.,* 2006). Indeed, a high degree of sharing of SVs between synapses has been reported (Darcy *et al.,* 2006a,b) and may be important for regulating synapse maintenance, efficacy, and plasticity (Staras, 2007). Elucidating the molecular mechanisms underlying SV recruitment and localization will therefore not only shed light on presynaptic assembly, but will also be informative with respect to mechanisms underlying presynaptic plasticity.

The cadherin–β-catenin adhesion complex has been shown to play a crucial role in the recruitment of SVs to synapses (Iwai *et al.,* 2002; Togashi *et al.,* 2002; Bamji *et al.,* 2003; Jungling *et al.,* 2006). We have previously demonstrated that some of the effects of cadherin on SV localization are attributed to the function of its intracellular binding partner, β-catenin (Bamji *et al.,* 2003, 2006). Indeed, in the absence of β-catenin, SVs do not cluster at synapses, resulting in an impaired response to prolonged repetitive stimulation. Domain analyses reveal that the armadillo domain of β-catenin (which binds cadherin), as well as its C-terminal PDZ-binding motif, are essential for proper SV localization, indicating that β-catenin mediates this effect by acting as a scaffold to tether PDZ protein(s) to cadherin clusters (Bamji *et al.,* 2003). Moreover, transient disruptions of cadherin–β-catenin interaction enhances the overall mobility of SVs and more specifically, enhances the efflux of SVs from established synapses (Bamji *et al.,* 2006). As regulation of SV localization is thought to be involved in presynaptic plasticity during development, these data suggest that the cadherin–β-catenin adhesion complex may play a role in this process. However, thus far, it is unclear how cadherin–β-catenin complexes regulate SV localization.

Scribble, a member of the LAP (leucine-rich repeats and PDZ domains) protein family (Yamanaka and Ohno, 2008), has been shown to localize to *Drosophila* neuromuscular junctions (NMJ; Mathew *et al.,* 2002), where it plays a role in regulating SV localization (Roche *et al.,* 2002). Loss-of-function mutations in *scribble* result in an accumulation of SVs at the NMJ and a decreased number of presynaptic active zones (Roche *et al.,* 2002). Moreover, several forms of plas-

This article was published online ahead of print in *MBC in Press* (http://www.molbiolcell.org/cgi/doi/10.1091/mbc.E08–12–1172) on May 20, 2009.

Address correspondence to: Shernaz X. Bamji (shernaz.bamji@ubc.ca).

ticity are drastically altered in *scribble* mutants, accompanied by impaired vesicle dynamics (Roche *et al.*, 2002). These results suggest that scribble is an essential regulator of SV turnover. A relationship between scribble and the cadherin–β-catenin complex has been demonstrated in various cell types and tissues (Navarro *et al.*, 2005; Nguyen *et al.*, 2005; Kamei *et al.*, 2007). For instance, scribble has recently been shown to exist in a complex with β-catenin and adenomatous polyposis coli (APC) in the mouse brain (Takizawa *et al.*, 2006). Our results suggest that scribble is recruited by β-catenin to presynaptic compartments, where it recruits SVs to developing synapses.

MATERIALS AND METHODS

RNA Interference Constructs and Recombinant DNAs

To suppress expression of endogenous scribble, three RNA interference (RNAi) constructs specifically against mouse scribble were transiently transfected into mouse hippocampal neurons. RNAi-1 and -2 are short hairpin RNA (shRNA) sequences corresponding to mouse scribble (GenBank accession no. NM_134089) nucleotides 3396-3416 and 1280-1300, respectively, and were expressed using the pRETROSUPER vector (Ludford-Menting *et al.*, 2005). RNAi-3 is a commercially available cocktail of three short interfering RNA (siRNA) oligonucleotides against mouse scribble (Santa Cruz Biotechnology, Santa Cruz, CA). An shRNA specifically against human scribble (GenBank accession no. NM_015356) nucleotides 1842-1862 was used as a control (RNAi-C; Dow *et al.*, 2007).

The Syn-GFP construct was a kind gift from T. Nakata (University of Tokyo, Tokyo, Japan). GFP-hScrib has been reported previously (Dow *et al.*, 2003). Red fluorescent protein (RFP)-hScrib construct was generated by replacing green fluorescent protein (GFP) with red fluorescent protein (RFP) at NheI/BsrGI sites of GFP-hScrib. Mouse β-catenin was cloned by standard PCR and inserted into the BamHI site of pGEX vector to generate glutathione *S*-transferase (GST)-β-cat, GST-β-cat ΔArm, and GST-β-cat ΔPDZb.

Neuron Cultures

Hippocampi from embryonic day 18 (E18) rat, E18 mouse, or postnatal day 1 (P1) B6.129-*Ctnnb1*^{tm2Kem}/KnwJ mouse (JAX Mice and Services, Bar Harbor, ME) were prepared as previously described (Xie *et al.*, 2000) and plated at a density of 130, 170, and 260 cells/mm^2, respectively. For Western analysis, hippocampal neurons were transfected with RNAis using the Amaxa Nucleofector System (Gaithersburg, MD) according to the manufacturer's instructions before plating. For all other analyses, neurons were transfected using Lipofectamine 2000 (Invitrogen Canada, Burlington, ON, Canada) at 7 days in vitro (DIV) and imaged at 10 DIV unless otherwise noted.

Semiquantitative RT-PCR

P1 mouse hippocampal cells were transfected with GFP plus scribble RNAi-C or RNAi-1 using Amaxa nucleofection. Total RNA was isolated using RNeasy Kit (Qiagen Canada, Mississauga, ON, Canada) and reverse transcribed using the SuperScript First Strand Synthesis system for RT-PCR kit (Invitrogen Canada). The resulting cDNA fragments were amplified by PCR using the following primers: mouse scribble primers (5′-CAG CCA AAG CTG AGC GAC G-3′; 5′-GAC AAA GGC AAG CGT CCA C-3′), mouse GAPDH primers (5′-CTG AAC GGG AAG CTC ACT-3′; 5′-GTC ATA CCA GGA AAT GAG C-3′), and GFP primers (5′-GTG AGC AAG GGC GAG GAG-3′; 5′-CTT GTA GTT GCC GTC GTC C-3′). PCR reaction was run on a 1% agarose gel and visualized by SYBR Safe DNA gel stain (Invitrogen Canada). The gel image was acquired using the AlphaImager Imaging system (Alpha Innotech, San Leandro, CA). To quantify band intensity, images were imported into NIH ImageJ (http://rsb.info.nih.gov/ij/), and the mean gray value was analyzed.

Immunohistochemistry

Neuron cultures were fixed in 4% paraformaldehyde/4% sucrose for 10 min, permeabilized in 0.1% Triton-X for 10 min, and blocked in 10% goat serum for 1 h at room temperature. Primary antibodies were applied in 1% goat serum overnight at 4°C, and secondary antibodies were applied in 1% goat serum for 1 h at room temperature. The following antibodies were used: primary antibodies: mouse anti-tau (Sigma, St. Louis, MO), mouse anti-synaptophysin (Sigma), rabbit anti-scribble (Santa Cruz Biotechnology), guinea pig anti-VGLUT-1 (Synaptic Systems, Goettingen, Germany), mouse anti-β-catenin (Zymed Laboratories, South San Francisco, CA), mouse anti-bassoon (Assay Designs, Ann Arbor, MI), mouse anti-PSD-95 (Affinity BioReagents, Golden, CO), and mouse anti-scribble (Dow *et al.*, 2003). Secondary antibodies: Alexa 488–, Alexa 633–, and Texas Red–conjugated goat anti-mouse or anti-rabbit (Molecular Probes, Eugene, OR).

FM 4-64 Analyses

FM 4-64 experiments were done as previously described (Gerrow *et al.*, 2006). Briefly, 15 μM FM 4-64 (Molecular Probes, Eugene, OR) was loaded for 30 s into presynatpic terminals using a hyperkalemic solution of 90 mM KCl in modified HBSS, where equimolar NaCl was omitted for final osmolality of 310 mOsm. Neurons were rinsed three times and maintained in HBSS without Ca^{2+} for imaging. ADVESAP-7 (1 mM, Sigma) was added to quench the nonspecific signal. Three images were captured every 30 s to confirm that the positive FM 4-64 sites were stationary presynaptic terminals. Unloading was done using the hyperkalemic solution described above, and neurons were rinsed three times with NeuroBasal media for continued imaging.

Immunoblot Analysis

Preparation of Protein Lysates. Brain tissues or cultured hippcampal neurons were homogenized in ~4 vol (wt/vol) of lysis buffer containing (50 mM Tris, pH 7.4, 150 mM NaCl, 1.0% NP-40, and 10% glycerol) and centrifuged at 14,000 × *g* for 30 min at 4°C.

Crude Synaptosomal Fraction (P2). E18 rats were decapitated, and brains were rapidly removed and placed in ice cold homogenization buffer (320 mM sucrose, 4 mM HEPES, and 1 mM EGTA). The tissue was homogenized in a homogenizer (Canadian Laboratory Supplies, Winnipeg, MB, Canada) by six gentle up-and-down strokes at 2300 rpm. The homogenate was centrifuged at 1312 × *g* for 10 min to remove nuclei and cell debris. The resulting supernatant was centrifuged at 14,481 × *g* for 15 min to remove small cell fragments and total soluble proteins. The resulting pellet was resuspended in homogenization buffer and centrifuged at 17,522 × *g* for 15 min to obtain the crude synaptosomal fraction, P2. P2 was resuspended in lysis buffer described above and used for immunoprecipitation and glutathione *S*-transferase (GST) pulldown assays.

Immunoprecipitation. P2 synaptosomal preparations were incubated overnight at 4°C with an anti-β-catenin antibody, an anti-scribble antibody, or preimmune serum. The following day, 50 μl of protein A/G-Sepharose (GE Healthcare, Chicago, IL) was added, and the bead-bound immunocomplexes were recovered after 2 h, washed four times with lysis buffer, solubilized with loading buffer, separated by SDS-PAGE, and analyzed by means of immunoblotting with antibodies against scribble, β-catenin, synaptophysin, or cadherin (Zymed Laboratories).

Western Blot Analysis. Proteins were visualized using enhanced chemiluminescence (Pierce Biotechnology, Rockford, IL) on a Bio-Rad Versadoc 4000 (Bio-Rad Laboratories, Mississauga, ON, Canada). The brightness and contrast of entire images was moderately adjusted using Photoshop (Adobe Systems Canada, Toronto, ON, Canada) after recommended, scientifically acceptable procedures, and no information was obscured or eliminated from the original (Rossner and Yamada, 2004).

Generation of GST Fusion Proteins and GST Pulldown Assays

GST-β-catFL, GST-β-cat ΔPDZb, and GST were expressed in *Escherichia coli* DH5α cells after induction with 0.1 mM isopropyl-β-D-1-thiogalactopyranoside for 3 h at 37°C. Bacteria were pelleted and lysed in PBS, 5 mM DTT, and 1 mM PMSF in the presence of protease inhibitors (Roche Diagnostics, Indianapolis, IN) by passing through French Press twice (Thermo Fisher Scientific, Waltham, MA). Fusion proteins were purified on glutathione Sepharose 4 Fast Flow (GE Healthcare) following the manufacturer's protocol. The amount of GST fusion protein input was verified by Coomassie blue staining.

For protein binding assays, Sepharose-bound GST fusions or GST were incubated with E18 synaptosomal preparations for 2 h at 4°C and followed by four washes with PBS. The proteins bound to the Sepharose beads were solubilized with loading buffer and loaded onto a SDS-PAGE. Proteins bound to the GST fusion protein were detected using antibodies against scribble and cadherin.

Confocal Imaging

Transfected hippocampal neurons were imaged using an Olympus Fluoview 1000 confocal microscope (10×/0.30 UPlan FL N; 20×/0.75 UPlan SApo; and 60×/1.4 Oil Plan-Apochromat, Melville, NY). All images in a given experiment were captured and analyzed with the same exposure time and conditions. To enhance visualization of the diffuse localization of Syn-GFP in scribble knockdown cells, the intensity levels of those representative pictures were enhanced using Adobe Photoshop.

Image Analysis and Quantification

Colocalization Analyses. Images of were analyzed using ImageJ with a colocalization plugin downloaded from the program's Web site (http://rsb.info.nih.gov/ij/plugins/colocalization.html). Points of colocalization

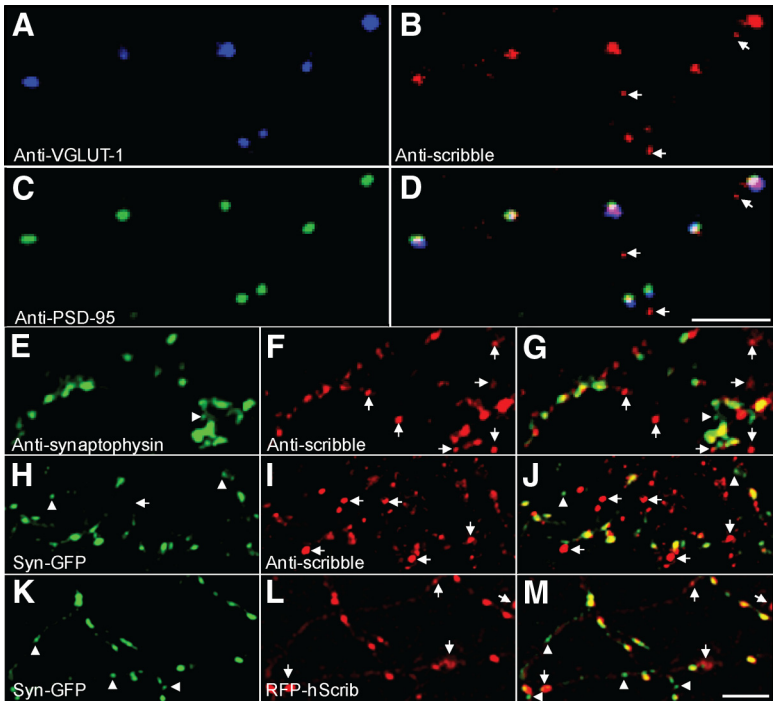

Figure 1. Scribble localizes to synapses. (A–M) Confocal images of 12 DIV hippocampal cultures. (H–M) To determine the subcellular localization of fluorescently tagged proteins in individual neurons, cells were transfected at <1% efficiency with Lipofectamine 2000 at 10 DIV. Endogenous scribble is localized in a punctate pattern and highly colocalizes with VGLUT-1 (A) and PSD-95 (B) puncta, indicating its localization at excitatory synapses (A–D). Scribble-positive puncta that do not colocalize with VGLUT-1/PSD-95 puncta are also observed (for examples see arrows). Endogenous scribble also colocalizes with synaptophysin (E–G), and Syn-GFP (H–J). RFP-hScrib is localized in a puncta pattern and colocalizes with Syn-GFP (K–M). Scribble-positive puncta that do not colocalize with synaptophysin (arrows), and synaptophysin puncta that do not colocalize with scribble (arrowheads) are observed (E–G). Similarly, the majority of Syn-GFP puncta colocalize with scribble (H–J). Scribble-positive puncta that do not colocalize with Syn-GFP represent immunostaining on cells not transfected with Syn-GFP (H–J; arrows). Arrows indicate RFP-hScrib puncta that do not colocalize with Syn-GFP (K–M). Scale bars, 5 μm.

were defined as regions greater than 4 pixels in size where the intensity ratio of the two channels was greater than 50. All the puncta were examined in a field. Numbers of colocalized puncta were expressed as a percentage of the total number of puncta, which were analyzed at threshold 85 (for VGLUT-1), 80 (for PSD-95), 80 (for scribble), 60 (for Synaptophysin), 80 (for β-catenin), 50 (for Syn-GFP), or 40 (for RFP-hScrib). To examine the percentage of synapses associates with scribble, a "mask" was made of VGULT-1 and PSD-95 overlay images, and the percentage was then determined by the presence of scribble on this mask.

Density Analyses. To determine the density of puncta along axons, puncta were manually counted, and the lengths of Syn-GFP–labeled axons were measured using ImageJ. The density was expressed as the number of puncta over 100-μm axon length.

Fluorescence Intensity Histogram. To examine the distribution of Syn-GFP fluorescence signal along the axon, a short line representing ~30 μm was drawn along the axon and through the major axis of Syn-GFP fluorescence signal. The distribution of fluorescence intensity along this line was determined by the Fluoview 1000 software, and the histogram was generated using Excel (Microsoft Canada, Mississauga, ON, Canada).

Coverage of Syn-GFP and RFP-hScrib Fluorescence. Variability in Syn-GFP and RFP-hScrib fluorescence can occur depending on the density of cells and the density of processes in a given region. To minimize variability, transfected neurons were identified, and the density of processes in the region was observed using brightfield. Images were obtained from regions with similar density of processes. With few exceptions, our cultures exhibit similar densities throughout the coverslip. To quantify the length of Syn-GFP and RFP-hScrib fluorescence signal, images were imported into ImageJ and the major axis lengths of Syn-GFP and RFP-hScrib fluorescence signal (Feret's diameter) were analyzed at a set threshold of 50 and minimum pixel size of 10. The distribution of Syn-GFP fluorescence signal was also expressed as the Syn-GFP fluorescence coverage, which represents the sum of the length of Syn-GFP fluorescence signal along a 10-μm axon length.

Intensity Analyses. Quantification of the intensity of Syn-GFP fluorescence at colocalized bassoon and PSD-95 sites were done using Image J. Sites of colocalized bassoon and PSD-95 puncta were first determined by the colocalization plug-in described above and saved as selections (a mask). The intensity of Syn-GFP fluorescence was quantified on bassoon/PSD-95 selections.

Puncta Size Analyses. To quantify the size of FM 4-64, bassoon, or β-catenin puncta along a single transfected neuron, a selection (mask) was initially made of the GFP signal). The area of the puncta within the selection was then quantified using ImageJ at threshold 100 (for FM 4-64), 80 (for β-catenin), and 100 (for bassoon).

RESULTS

Scribble Interacts with β-Catenin and Localizes at Synapses

Drosophila scribble has been implicated in the development of synapse structure and function (Roche *et al.*, 2002). The mammalian homolog of scribble has a primary structure similar to that of its fly homolog (Santoni *et al.*, 2002), and localizes to distinct regions in the brain, including the hippocampus (http://www.brain-map.org/). However the function of scribble in neurons remains unknown. To determine the distribution of scribble in hippocampal neurons, 10 DIV primary hippocampal cultured neurons were immunostained for scribble. Scribble immunoreactivity was observed throughout the cell, being localized to both dendrites and axons (Supplementary Figure S1). Previous work has demonstrated that scribble is localized to synapses in cultured cerebellar neurons (Audebert *et al.*, 2004; Takizawa *et al.*, 2006). Analysis of hippocampal cultures demonstrates a similar synaptic distribution for scribble (Figure 1, A–D), whereby 84.8% of excitatory synapses, identified by colocalization of the presynaptic vesicular glutamate transporter, VGLUT-1, and the excitatory postsynaptic marker, PSD-95, were associated with scribble immunoreactive puncta (Table 1). Scribble puncta that are not associated with VGLUT-1 and PSD-95 may represent populations at inhibitory synapses or at nonsynaptic sites (Figure 1, B and D, arrows). Moreover, the majority of synaptophysin, an integral synaptic vesicle (SV) marker, colocalizes with scribble (Figure 1, E–G, Table 1). Scribble-positive sites that are not associated with synaptophysin may represent mobile scribble clusters or scribble clusters that are at nascent synapses before the recruitment of synaptic vesicles.

GFP-tagged synaptic vesicle marker proteins have been widely used to mark presynaptic sites in vertebrates and do not compromise the secretory physiology of the synapse (Sankaranarayanan and Ryan, 2000). Moreover, our work has previously demonstrated that the pattern of synapto-

Table 1. Analysis of scribble localization at synapses

Condition	Average ± SE	N
% VGLUT-1/PSD-95 colocalized with scribble	84.8 ± 1.82	21 images, 2 cultures
% synaptophysin colocalized with scribble	68.3 ± 5.69	12 images, >3 cultures
% Syn-GFP colocalized with scribble	74.6 ± 9.54	10 cells, 3 cultures
% Syn-GFP colocalized with RFP-hScrib	75.7 ± 6.53	9 cells, >3 cultures
Density of scribble immunoreactive puncta/100 μm	8.14 ± 1.19	10 cells, 3 cultures
Density of RFP-hScrib puncta/100 μm	9.56 ± 1.23	11 cells, >3 cultures
% β-Catenin colocalized with scribble	72.0 ± 3.10	12 images, >3 cultures
% β-Catenin/scribble colocalized with bassoon	87.9 ± 1.31	10 images, 2 cultures
% bassoon colocalized with β-catenin/scribble	70.6 ± 1.65	10 images, 2 cultures

physin-GFP (Syn-GFP) expression is comparable to that of endogenous SV proteins (Bamji *et al.*, 2003). Endogenous scribble puncta were found to colocalize with Syn-GFP to approximately the same degree, further demonstrating the faithful use of this tagged marker (Figure 1, H–J, Table 1). To determine whether RFP-conjugated human scribble (RFP-hScrib) is appropriately expressed, neurons were cotransfected with RFP-hScrib and Syn-GFP. The percent colocalization of RFP-hScrib and Syn-GFP was highly similar to that observed with endogenous scribble and synaptophysin (Figure 1, K–M, Table 1). Finally, the density of RFP-hScrib clusters was similar to that of endogenous scribble (Table 1, $p > 0.05$), and RFP-hScrib was found associated with endogenous synaptophysin clusters (data not shown). Thus, our data indicate that Syn-GFP and RFP-hScrib are faithful markers for assaying appropriate localization patterns of the corresponding endogenous proteins.

We next examined the association of endogenous scribble and β-catenin in neurons. Immunohistochemical analysis demonstrated that a large proportion of β-catenin puncta colocalize with scribble puncta. These colocalized clusters were highly enriched at bassoon immunoreactive sites, suggesting that scribble colocalizes with β-catenin at synapses (Figure 2, A–E, Table 1). To further demonstrate that scribble associates with β-catenin at synapses, crude synaptosomal fractions from E18 brains were prepared and immunoprecipitated with antibodies against scribble and β-catenin. Coimmunoprecipitation assays demonstrate that scribble associates with β-catenin and cadherin at synapses (Figure 2F). The interaction between β-catenin and scribble was further confirmed using GST pulldown assays (Figure 2G).

β-Catenin consists of three domains: an N-terminal domain that interacts with α-catenin, a central domain of 12 armadillo repeats that binds to cadherin and LEF/TCF transcription factors (Daniels *et al.*, 2001; Ivanov *et al.*, 2001), and a C-terminal domain that interacts with transcriptional regulators and contains a PDZ-binding motif (Perego *et al.*, 2000). Our previous work demonstrated that the PDZ-binding motif is essential for the clustering of SVs at synaptic junctions (Bamji *et al.*, 2003). To investigate whether this domain is important for the interaction between β-catenin and scribble, β-catenin deletion mutant lacking the PDZ-binding motif (GST-β-catΔPDZb) was generated (Figure 2G). Full-length β-catenin (GST-β-cat FL) was able to pulldown scribble and cadherin from synaptosomal fractions. In contrast, deletion of the C-terminal 10 amino acids containing the PDZ-binding motif abolished the association between β-catenin and scribble. As expected, GST-β-catΔPDZb was able to pulldown cadherin from synaptosomal fractions (Figure 2G). Together, this demonstrates that scribble asso-

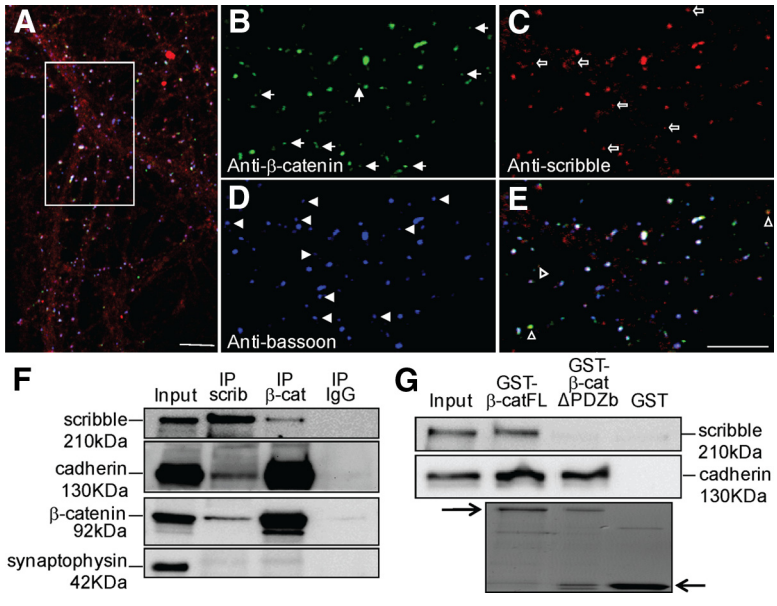

Figure 2. Scribble associates with β-catenin at synapses. (A–E) Confocal images of 12 DIV hippocampal cultures demonstrating colocalization of scribble, β-catenin, and the presynaptic marker, bassoon. Higher magnifications of the inset from A are shown in B–E. The majority of scribble puncta colocalized with β-catenin and bassoon. β-catenin puncta that do not colocalize with scribble (arrows), scribble puncta that do not colocalize with β-catenin (open arrows), and bassoon puncta that do not associate with β-catenin and scribble (arrowheads) are observed. Colocalized scribble and β-catenin puncta that are not associated with bassoon positive sites are also observed (open arrowheads). (F and G) Scribble and β-catenin can be coimmunoprecipitated from synaptosomal fractions. Synaptosomal fractions from E18 brains were immunoprecipitated using β-catenin or scribble antibodies and separated by SDS-PAGE, and immunoblots probed with antibodies specific to scribble, β-catenin, synaptophysin, or cadherin. The input lane corresponds to 40 μg of the crude synaptosomal fraction, P2. Rabbit IgG was used as a control. Scribble and β-catenin were coimmunoprecipitated with one another and with cadherin, but not with the synaptic protein, synaptophysin, indicating the specificity of the immunoprecipitation. N = 2 different preparations. (G) Synaptosomal fractions from E18 brains were affinity purified with GST-β-cat FL, GST-β-cat ΔPDZb, or GST alone bound to glutathione-Sepharose beads. Coomassie blue staining was used to verify the levels of GST and GST fusion proteins used for GST pulldown assay (arrows). Bound proteins were eluted, and blots were probed with anti-scribble or anti-cadherin. Scale bars, 5 μm.

ciates with cadherin and β-catenin at synapses via the PDZ-binding motif of β-catenin.

SVs Are Mislocalized in Hippocampal Neurons Lacking Scribble

To study the role of scribble at synapses, scribble protein levels were attenuated in hippocampal neurons using RNAi. To minimize possible "off-target" effects, two shRNAs (RNAi-1 and -2) and one cocktail of three siRNA oligonucleotides (RNAi-3) were used. The efficacy of the RNAis was examined using Western blot analysis. Although the efficiency of transfection was on average only 35.9 ± 2%, a significant decrease in scribble protein levels was observed in cultures transiently transfected with RNAi-1, -2, or -3, compared with cultures transfected with control RNAi (RNAi-C; Figure 3, A and B). In contrast, β-catenin levels remained similar in scribble RNAi-expressing cells (Figure 3A). (It is important to note that Figure 3B represents raw data and has not been normalized for transfection efficiency.) Similarly, quantitative RT-PCR revealed significant decreases in scribble transcripts in cultures transfected with RNAi (Supplementary Figure S2). The efficiency of scribble depletion was similar among all three RNAi treatments and was used interchangeably in subsequent experiments. To further confirm the knockdown of scribble protein in neurons expressing RNAi, cultured hippocampal neurons were transfected with either RNAi-C or each one of the three RNAis and immunolabeled for scribble. Cells were cotransfected with Syn-GFP to mark RNAi-transfected neurons. At low magnifications, expression levels of scribble in cell bodies of control cells were abundant (Figure 3C, D asterisks), whereas in cells expressing RNAi-1, somatic scribble levels were dramatically decreased (Figure 3, E and F, asterisks). This was consistently observed in neurons expressing each of the three RNAis, indicating an effective knockdown of scribble in neuronal cultures.

Interestingly, the pattern of Syn-GFP expression in RNAi-expressing neurons was altered compared with control neurons. In wild-type cells, discrete Syn-GFP puncta were observed along the axon (Figures 3D′ and 4, A and B). In contrast, in scribble RNAi-expressing cells, discrete Syn-GFP puncta were not observed. (Figures 3F′ and 4, F and G). To

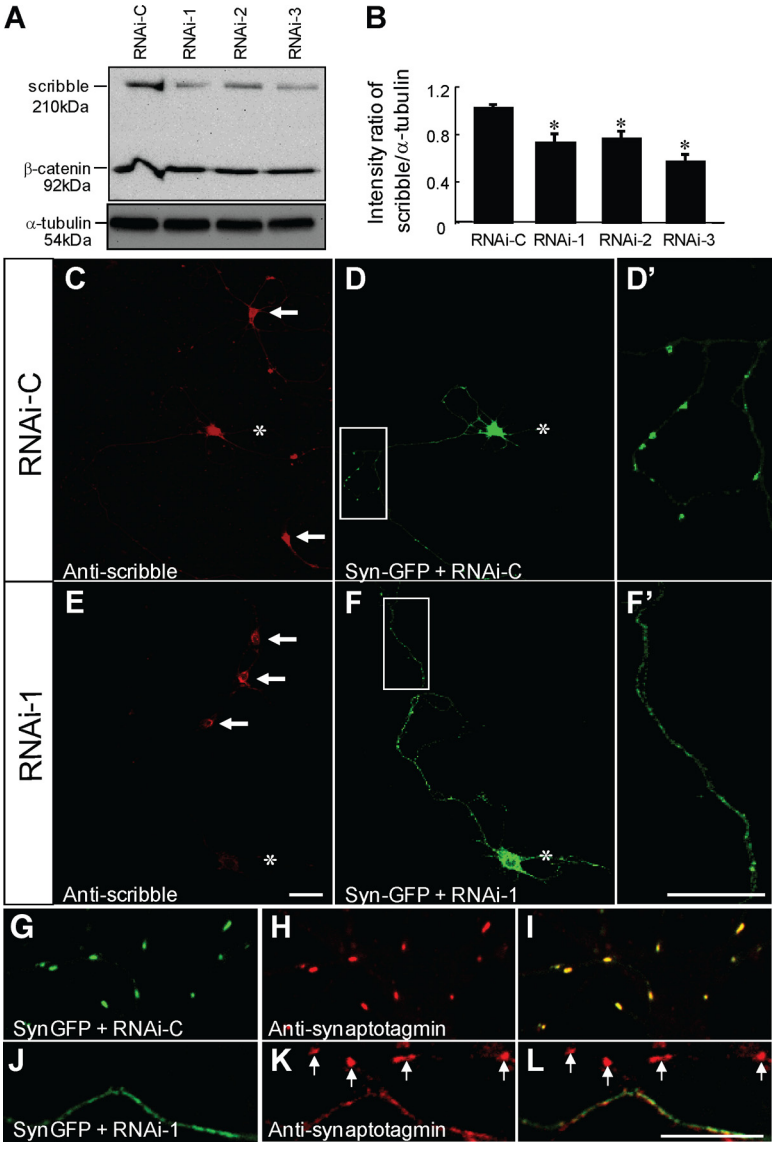

Figure 3. RNAi-mediated knockdown of scribble protein levels in primary neurons. (A and B) Neurons were transfected with control RNAi (RNAi-C), or three distinct scribble RNAis (RNAi-1-3) with ~35% transfection efficiency using the Amaxa nucleofector system. Immunoblot analysis revealed a decrease in scribble protein levels in all three RNAi-expressing cultures, whereas β-catenin levels remained constant. (B) Quantification of immunoblots represents raw data and has not been normalized for transfection efficiency (35.9 ± 2%). N = 3 immunoblots from three separate cultures. *$p < 0.05$ using Student's *t* test. (C–L) Confocal images of 10 DIV hippocampal neurons cotransfected using Lipofectamine 2000 (<1% transfection efficiency) with Syn-GFP plus either RNAi-C (D and G) or RNAi-1 (F and J) and immunostained for scribble (C and E) or synaptotagmin (H and K). The neuron expressing RNAi-1 shows a clear reduction in scribble immunostaining in the cell body (E) compared with RNAi-C–expressing cell (C). *, transfected neurons; arrows, untransfected neurons. Syn-GFP is punctate in RNAi-C–expressing cells (D′ and G), but more diffusely localized in cells expressing RNAi-1 (F′ and J). (G–L) Endogenous synaptotagmin is diffusely expressed in RNAi-1–expressing cells. In RNAi-expressing cells Syn-GFP and synaptotagmin are colocalized and display a punctate distribution (G–I). In contrast, in neurons expressing RNAi-1, both Syn-GFP and synaptotagmin are more diffusely distributed (J–L). Synaptotagmin-positive puncta that do not colocalize with Syn-GFP represent immunostaining on cells not transfected with Syn-GFP and RNAi-1. Scale bars, 20 μm.

confirm the distribution of SVs in RNAi-transfected cells, cultures were immunostained with synaptotagmin, another integral SV marker. Synaptotagmin expression appeared similar to that of Syn-GFP, with fewer large immunopositive clusters along RNAi-expressing axons (Figure 3, J–L).

To further investigate the pattern of SV localization in neurons, and specifically its localization at synaptic sites, cells were transfected with Syn-GFP and RNAi-C or each of the three RNAis and immunostained with bassoon and PSD-95 to label pre- and postsynaptic sites, respectively. In control neurons, the fluorescence intensity of the Syn-GFP–positive puncta was high, as observed in the pseudocolored, low-magnification image (Figure 4A) and in the intensity distribution histogram (Figure 4K). Discrete fluorescence intensity peaks representing individual Syn-GFP puncta were observed, and the level of fluorescence intensity between peaks (interpunctal intensity) was relatively low (Figure 4, A and K). These Syn-GFP–positive puncta were localized to synapses as observed by its colocalization with PSD-95 and bassoon (Figure 4, B–E). In contrast, in RNAi-expressing cells, the fluorescence intensity distribution of Syn-GFP was relatively uniform along the axon, with an overall increase in basal intensity compared with the interpunctal intensity of wild-type cells (Figure 4, F and L). Although Syn-GFP fluorescence was more diffusely distributed along the axon, PSD-95 and bassoon colocalization (synapses) was still evident in these cells (Figure 4, G–J).

We next measured synaptophysin levels to ensure that changes in the pattern of Syn-GFP distribution in scribble knockdown cells were not due to overall changes in synaptophysin expression. Both synaptophysin and β-catenin levels remained similar in scribble RNAi-expressing cells compared with control (Figure 4M), suggesting that attenuation of scribble perturbs the distribution of SV clusters,

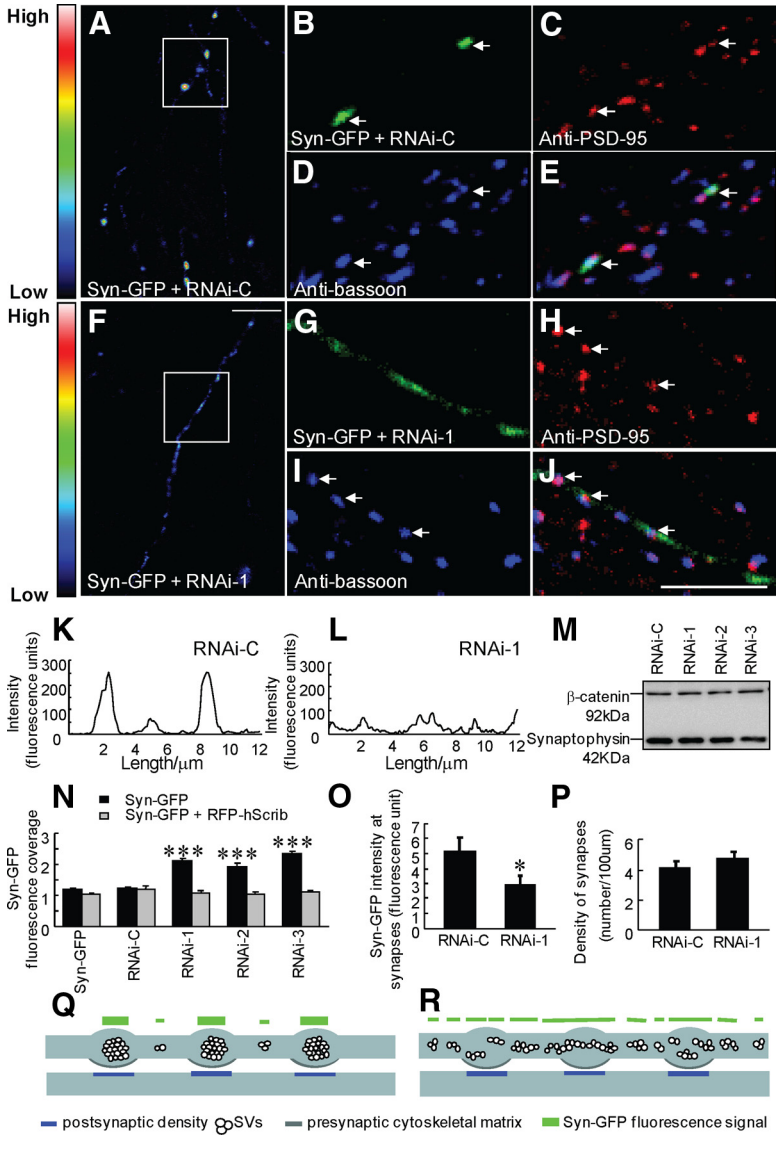

Figure 4. SVs are more diffusely distributed along the axon in neurons expressing scribble RNAi constructs. (A–J) Confocal images of 10 DIV hippocampal neurons cotransfected with Syn-GFP plus scribble RNAis using Lipofectamine 2000 (<1% transfection efficiency) and immunostained for bassoon and PSD-95. Synapses were defined as regions where bassoon and PSD-95 puncta colocalized. (A and F) Images of neurons transfected with RNAi-C (A) and RNAi-1 (F) and pseudocolored for fluorescence intensity. Insets from A and F are shown in higher magnification (B–E and G–J) and selected for histogram analyses (K and L). In RNAi-C–expressing neurons, Syn-GFP is punctate and colocalizes with PSD-95 and bassoon (B–E, arrows). In RNAi-1–expressing neurons, Syn-GFP fluorescence is more diffusely distributed along the axon; however, discrete bassoon and PSD-95 colocalization is still observed (G–J, arrows). Immunopositive bassoon and PSD-95 puncta that do not colocalize with Syn-GFP may represent immunostaining on untransfected neurons. (K and L) Histograms of Syn-GFP fluorescence intensity along a selected axon length in neurons expressing RNAi-C (A and B) or RNAi-1 (F and G) demonstrate that the distribution of Syn-GFP fluorescence is more uniform in scribble knockdown cells and lack distinct punctal and interpunctal regions. (M) Using the Amaxa nucleofector system, neurons were transfected with control RNAi (RNAi-C) or scribble RNAis (RNAi-1-3), and the expression level of synaptophysin and β-catenin was analyzed using Western blot. Despite the fact that synaptophysin protein levels are similar in cultures transfected with RNAi-C and RNAi-1-3 (M), the coverage of Syn-GFP along the axon (the sum of the length of Syn-GFP fluorescence signal per 10 μm axon length ± SE) is greater in RNAi-expressing cells (N). N = 30–60 cells and >2000 puncta from more than three separate cultures. ***$p < 0.0001$ using Student's t test. (O) A significant decrease in the average intensity of Syn-GFP fluorescence at sites of bassoon/PSD-95 colocalization was observed in RNAi-expressing cells. N = >23 cells and 106–158 colocalized bassoon and PSD-95 puncta from at least three separate cultures. *$p > 0.05$ using Student's t test. (P) The density of bassoon/PSD-95 clusters along transfected axons (the average number of colocalized immunopositive puncta per 100 μm of axon length ± SE), was similar in control and RNAi-expressing cells. (Q and R) Schematic of the effect of scribble knockdown on SV localization. (Q) In wild-type neurons, SV clusters are localized to synapses, and some clusters are also observed in perisynaptic regions. (R) In scribble knockdown cells, SVs are more diffusely distributed along the axon and less SVs are accumulated at synapses. Green bars above each axon mark the length of SV clusters, and thickness reflects the relative intensity of Syn-GFP clusters. Although the number of SVs in wild-type and knockdown cells are similar, the Syn-GFP fluorescence coverage is greater in knockdown cells, highlighting the diffuse distribution of SVs along the axon. Scale bars, 5 μm.

while leaving the overall expression of SV proteins undisturbed.

Variability in the "punctate-ness" of Syn-GFP was observed in RNAi-expressing cells. To determine the distribution of vesicles along the axon, the Feret's diameter (defined as the greatest distance possible between any two points along the boundary of a region of interest, hereafter called the "length") of the Syn-GFP fluorescence signal was determined as described previously (Bamji *et al.*, 2003). To avoid bias, all transfected neurons on each coverslip were imaged and quantified. A 28.6–34.4% increase was observed in the average length of Syn-GFP fluorescence signal in knockdown cells compared with wild-type. Although the increase was significant, the difference between wild-type and knockdown cells was minimized due to an increased density of small Syn-GFP puncta in knockdown cells which we believe arise from small clusters of SVs that are not retained at synapses. To address this, the sum of the length of Syn-GFP fluorescence signal per 10 μm axon length (hereafter referred to as the "coverage") was used to represent the distribution of SVs along the axon (Figure 4N). No significant difference was seen in Syn-GFP coverage between neurons expressing Syn-GFP alone and Syn-GFP plus RNAi-C. In contrast, the coverage of Syn-GFP along the axon was over twofold greater in RNAi-expressing neurons compared with neurons expressing RNAi-C. The magnitude of the phenotype was similar for all three RNAis. Importantly, coexpression of RFP-hScrib that is insensitive to our RNAis rescued this phenotype, indicating that the observed effects were primarily due to specific interference with scribble function (Figure 4N).

To further assess the distribution of SVs at synapses, the intensity of Syn-GFP fluorescence at synapses (defined here as points of colocalization between PSD-95 and bassoon) was quantified. A significant decrease in Syn-GFP fluorescence intensity at synapses was observed in RNAi-transfected cells compared with control cells (Figure 4O), suggesting that SV number is specifically diminished at synaptic junctions upon scribble knockdown. Synapse number was also quantified by counting the density of bassoon-positive puncta that colocalized with PSD-95 in control and RNAi-transfected cells, and no significant difference was observed (Figure 4P).

To determine the role of scribble on presynaptic development beyond its role in SV localization, the expression pattern of the presynaptic cytoskeletal matrix protein, bassoon, was examined. Bassoon is recruited to synapses in large dense-core vesicles along with other components of the active zone, including piccolo, N-cadherin, syntaxin, SNAP-25, and chromogranin B, independently of the vesicles that transport SV proteins to synapses (Zhai *et al.*, 2001). The density, size, and intensity of endogenous bassoon was similar between control and scribble RNAi-expressing neurons (Supplementary Figure S3). These data suggest that scribble is involved in some, but not all steps, of synapse assembly.

Taken together, our results demonstrate an important role for scribble in localizing SVs to synapses. In cells expressing scribble RNAi, discrete SV clusters are rarely observed, and the intensity of Syn-GFP fluorescence at synapses significantly decreases. Interestingly, scribble knockdown does not appear to affect the localization of other presynaptic proteins such as bassoon or the density of synapses along the axon. This phenotype is very similar to the observation in β-catenin knockout neurons (Bamji *et al.*, 2003).

SV Recycling Defects in Cultured Hippocampal Neurons Lacking Scribble

Vesicle recycling is required to maintain SV pools and enable efficient neurotransmission at synapses (Sudhof, 2004; Schweizer and Ryan, 2006). To determine whether the de-

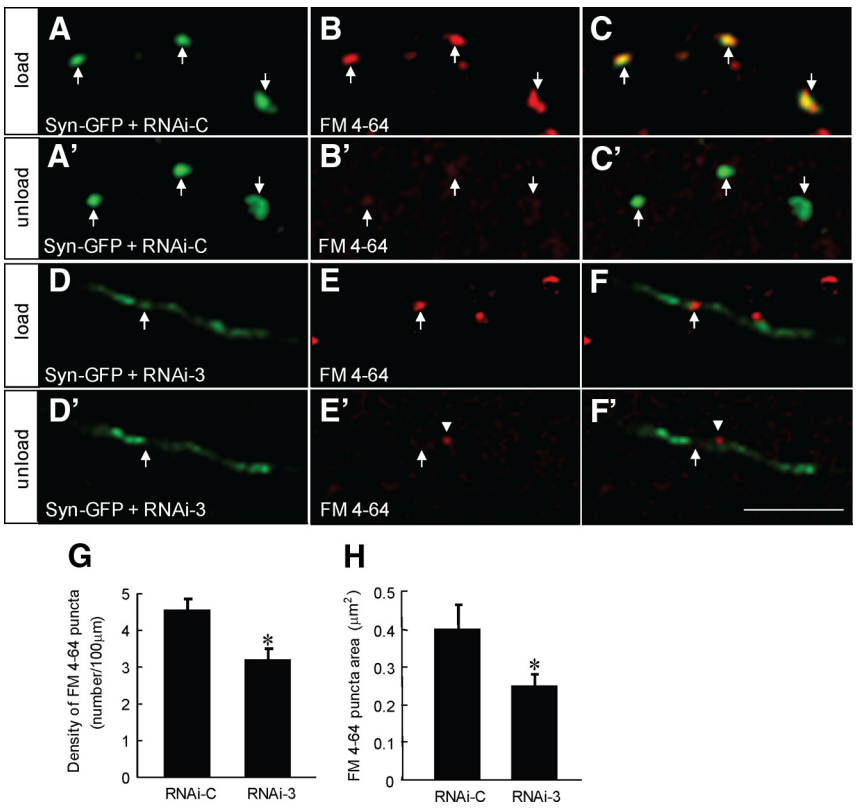

Figure 5. Deficits in SV recycling after scribble knockdown. (A–F) Confocal images of 10 DIV neurons transfected with Syn-GFP and the indicated RNAi using Lipofectamine 2000 (<1% transfection efficiency). Neurons were loaded with FM 4-64, and three images were captured every 30 s to confirm that the positive FM 4-64 sites were stationary presynaptic terminals. Arrows indicate FM 4-64–positive sites on transfected axons. FM dyes were then unloaded to demonstrate specificity (A′–F′). (F′) The FM 4-64–positive site (arrowhead) not observed in dye-"load" image (E), but observed following dye-"unload" (E′) most likely represents a mobile FM 4-64–positive puncta on an untransfected neuron. The FM 4-64 cluster in the transfected neurons (arrow) is not observed after de-staining. The density (G) and size (H) of FM 4-64-positive puncta ± SE were reduced in cells expressing RNAi-3 compared with control. N = 17 cells and >85 FM-4-64 puncta from more than three separate cultures. *$p < 0.05$ using Student's t test. Scale bar, 5 μm.

fects in vesicle localization in scribble knockdown cells are associated with impaired presynaptic function, the efficiency of vesicle recycling was studied by stimulating neurons with a high-K^+ solution in the presence of FM 4-64, a fluorescent dye that marks sites of endocytosis. In control cultures, uptake of FM 4-64 was observed at Syn-GFP sites (Figure 5, B and C). However, in cultures expressing scribble RNAi, this uptake was strongly suppressed, with greatly reduced density and size of FM 4-64–positive puncta compared with control cells (Figure 5, E–G). To confirm that this was a synaptic activity-dependent phenomenon, we assessed FM 4-64 unloading by restimulating labeled neurons. This treatment almost completely removed FM 4-64 dye in both control and experimental cultures (Figure 5, B′ and E′), suggesting activity-dependent vesicle recycling.

β-Catenin Localizes Scribble to Synapses

Our previous work has demonstrated a role for β-catenin in the localization of SVs (Bamji *et al.*, 2003). In light of our above results showing that scribble is also required for normal localization of SVs and that scribble and β-catenin exist in complex with each other, we next determined whether scribble acts in concert with β-catenin to localize SVs. First, the localization of β-catenin in scribble knockdown neurons was examined. In wild-type cells, endogenous β-catenin displayed a punctate expression pattern and colocalized with Syn-GFP (Figure 6, A–C). In scribble knockdown cells, there was a diffuse pattern of Syn-GFP expression; however the β-catenin remained punctate (Figure 6, D–F). Moreover, the density of β-catenin along the axon, as well as the area of β-catenin, remained similar in control and scribble RNAi-transfected cells (Figure 6, G and H). This suggested that the localization of β-catenin at synapses is not dependent on scribble.

We next tested the role of β-catenin in the recruitment and synaptic localization of scribble. Hippocampal neurons prepared from B6.129-*Ctnnb1*^{tm2Kem}/KnwJ mice (homozygous *β-catenin* flox mice) were transfected with a vector expressing the Cre recombinase to ablate *β-catenin*. This methodology has previously been shown to efficiently ablate *β-catenin* in vitro (*Bamji et al.*, 2003). In control cells, RFP-hScrib was expressed in a punctate pattern and colocalized with Syn-GFP and PSD-95 at synapses (Figure 7, A–D). In contrast, expression of the Cre recombinase in *β-catenin flox* neurons resulted in the expected diffuse pattern of Syn-GFP expression, as well as a diffuse pattern of RFP-hScrib expression (Figure 7, E–H). Indeed, the average length of RFP-hScrib fluorescence along the axon was significantly greater in cells lacking β-catenin (Figure 7O). Interestingly, PSD-95 puncta at postsynaptic sites apposed to transfected axons remained punctate (Figure 7G).

We have demonstrated that the PDZ-binding motif of β-catenin is important for the interaction between β-catenin and scribble (Figure 2G). To test whether the PDZ-binding motif is important for the synaptic localization of scribble, neurons were transfected with either β-cat FL or β-catΔPDZb, plus Syn-GFP and RFP-hScrib. In cells expressing β-cat FL, Syn-GFP and RFP-hScrib had a punctate distribution and were largely colocalized, similar to that observed with endogenous synaptophysin and scribble proteins (Figures 7, I–K, and 1, E–G). As previously demonstrated, cells expressing β-catΔPDZb exhibited a diffuse pattern of Syn-GFP expression (Figure 7L; Bamji *et al.*, 2003). Interestingly, in these cells, scribble was also diffusely distributed along the axon (Figure 7, M and P). These data suggest that β-catenin plays an important role in localizing scribble to synaptic sites and that scribble acts downstream of β-catenin to localize SVs.

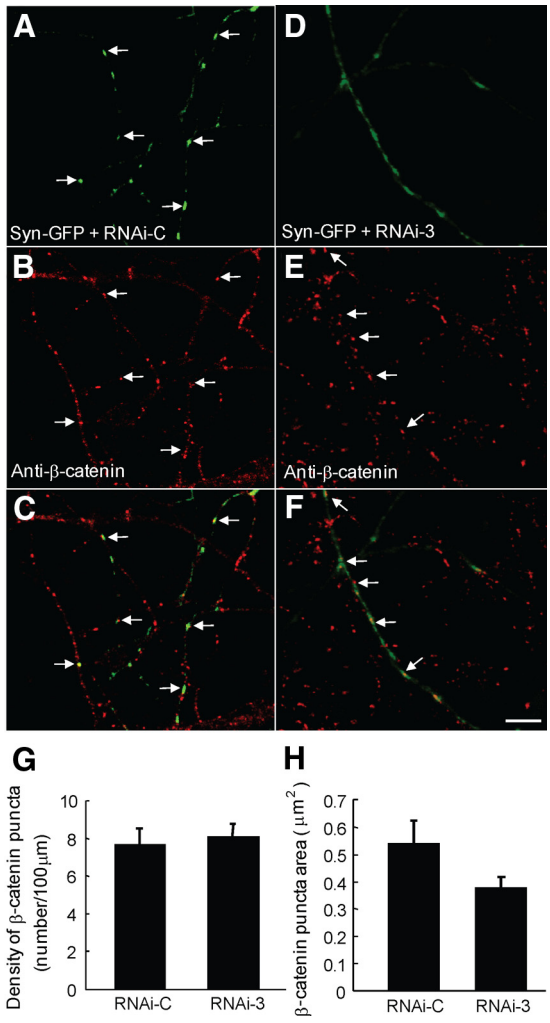

Figure 6. β-Catenin localization is not affected in scribble RNAi-expressing cells. (A–F) Confocal images of 10 DIV hippocampal neurons transfected with Syn-GFP and RNAi-C (A–C) or RNAi-3 (D–F) using Lipofectamine 2000 (<1% transfection efficiency) and immunostained for β-catenin. Syn-GFP puncta colocalize with β-catenin puncta in cells expressing RNAi-C (B and C; arrows). Neurons expressing RNAi-3 exhibit a diffuse pattern of Syn-GFP (D); however, β-catenin expression remains punctate (E and F; arrows). The average density (G) and size (H) of β-catenin puncta ± SE is similar in control and RNAi-expressing cells. N > 10 cells and >250 puncta from three cultures. $p > 0.05$ using Student's *t* test. Scale bar, 10 μm.

DISCUSSION

Increasing evidence suggests that there is a strong correlation between the number of SVs localized at presynaptic compartments and synaptic efficacy (Murthy *et al.*, 2001; Cabin *et al.*, 2002; Taschenberger *et al.*, 2002; Bamji *et al.*, 2003; Thiagarajan *et al.*, 2005). As synapses mature, vesicle pool size and exocytotic efficiency (amount of exocytosis per Ca^{2+} influx) increases, resulting in more effective transmission after bursts of neuronal activity (Taschenberger *et al.*, 2002). Evidence suggests that altering neuronal activity can impact the number of SVs localized to the presynaptic zone of

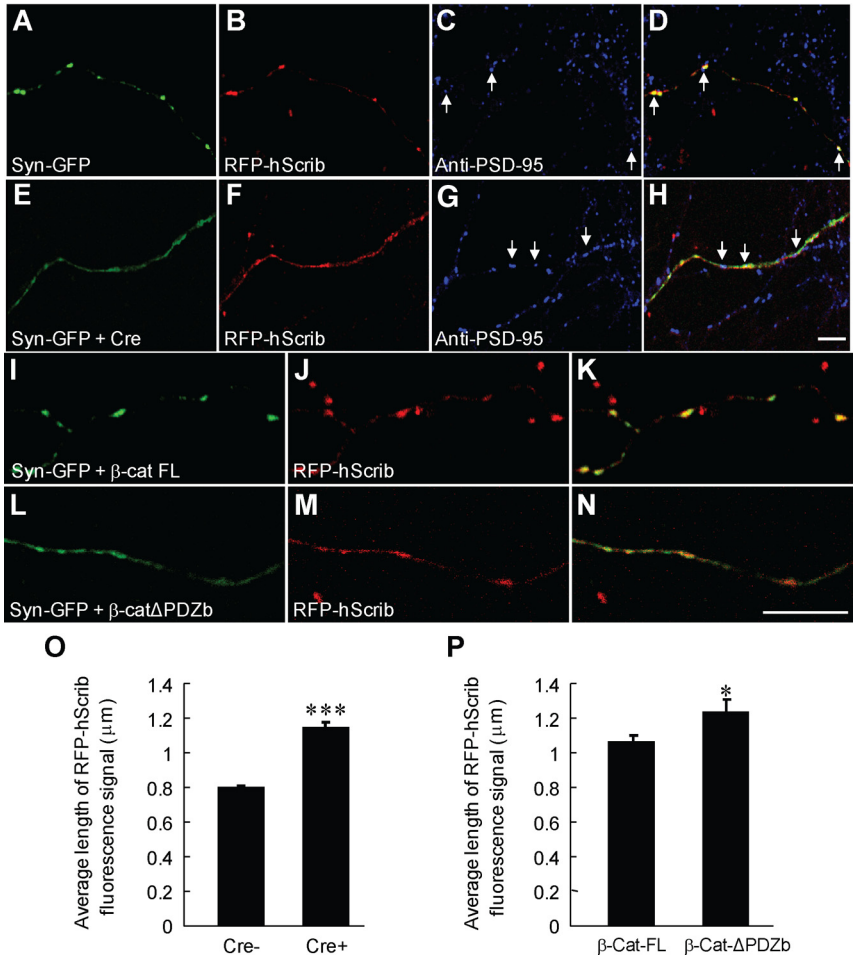

Figure 7. Scribble is diffusely distributed long the axon in cells lacking β-catenin. (A–H) Hippocampal neurons cultured from 10 DIV B6.129-Ctnnb1^{tm2Kem}/KnwJ (homozygous β-catenin flox) mice were cotransfected using Lipofectamine 2000 (<1% transfection efficiency) with Syn-GFP and RFP-hScrib (A–D) or Syn-GFP, RFP-hScrib, and a construct expressing the Cre recombinase to ablate β-catenin (E–H). Confocal images demonstrate that Syn-GFP and RFP-hScrib are colocalized and are apposed to postsynaptic PSD-95 at synapses in control cells (C and D; arrows). Neurons expressing the Cre recombinase exhibit a diffuse expression of Syn-GFP and RFP-hScrib (E and F), whereas PSD-95 expression remains punctate (G and H; arrows). Immunopositive PSD-95 puncta that do not colocalize with Syn-GFP may represent immunostaining on neurons that are not transfected. (I–N) Confocal images of 10 DIV hippocampal neurons transfected with Syn-GFP and RFP-hScrib plus either β-cat FL (I–K) or β-catΔPDZb (L–N). In β-cat FL–expressing neurons, Syn-GFP puncta largely colocalize with RFP-hScrib puncta (I–K; arrows), whereas cells expressing β-catΔPDZb exhibit a diffuse pattern of Syn-GFP and RFP-hScrib expression (L–N). The normalized average coverage of RFP-hScrib along the axon ± SE is greater in cells lacking β-catenin (Cre+ cells) (O) and in cells expressing β-catΔPDZb (P), indicating a more diffuse distribution along the axon. $N > 7$ cells and >500 puncta from three different cultures. *$p < 0.05$, ***$p < 0.0001$ using Student's t test. Scale bars, 10 μm.

mature synapses. For example, when hippocampal synapses in culture are pharmacologically silenced for several days, synaptic strength increases. Among changes in other synaptic components, this corresponds to an increase in the total number of docked vesicles and the total number of vesicles per synapse (Murthy *et al.*, 2001), as well as an increase in the rate of vesicle turnover (Thiagarajan *et al.*, 2005). Changes in the number of SVs per synapse can also alter synaptic efficacy. Indeed, in both α-synuclein (Cabin *et al.*, 2002) and β-catenin (Bamji *et al.*, 2003) knockout mice, there is a decrease number of total SVs per synapse, and a concomitant impairment in the synaptic response to prolonged repetitive stimulation. Understanding the mechanism of SV localization to synapses is therefore essential to our understanding of synapse development and function.

Recent studies demonstrate that the cadherin–β-catenin adhesion complex plays a central role in recruiting and retaining SVs to synapses (Iwai *et al.*, 2002; Togashi *et al.*, 2002; Bamji *et al.*, 2003, 2006; Bamji *et al.*, 2006). β-Catenin was shown to act downstream of cadherin to mediate SV localization (Bamji *et al.*, 2003). Because both the internal armadillo repeats that bind cadherin and the PDZ-binding motif of β-catenin are important for vesicle localization, β-catenin is believed to mediate SV clustering by acting as a scaffold (Bamji *et al.*, 2003). In this study, we identify the PDZ protein downstream of β-catenin that localizes SVs to synapses. We demonstrate that β-catenin recruits scribble to synapses and forms a complex with scribble through its C-terminal PDZ-binding motif. Scribble, in turn, regulates the recruitment and localization of SVs.

Scribble Interacts with β-Catenin at Synapses

The present study indicates an interaction between scribble and β-catenin. Indeed, scribble can be coimmunoprecipitated with β-catenin from synaptosomal preparations and largely colocalizes with β-catenin at synapses in cultured hippocampal neurons. GST pulldown assays showed that the PDZ-binding motif at the C-terminus of β-catenin is essential for this interaction. Our data demonstrating that β-catenin's PDZ-binding motif is important for synaptic localization for scribble and SV suggests that scribble could be the downstream regulator to mediate β-catenin's role in SV localization.

It is still unclear, however, whether this interaction is direct or indirect. Scribble has four PDZ domains, and it is possible that one or more of these directly interact with β-catenin PDZ-binding domain. Indirect interactions are also plausible. For example, it has been suggested that scribble and β-catenin may interact indirectly via their association with APC (Takizawa *et al.*, 2006). We do not believe that APC is acting as an intermediary for the association between scribble and β-catenin at synapses because β-catenin interacts with APC via its armadillo domain (Su *et al.*, 1993), and our data suggest the PDZ-binding motif of β-catenin is important for its association with scribble.

Role of Scribble in the Synaptic Localization of SVs

Interestingly, the role of β-catenin and scribble in regulating SV localization is independent of the initial steps of presynaptic development (Zhai *et al.*2001), and bassoon remains punctate in β-catenin knockout cells (Bamji *et al.*, 2003) and scribble knockdown cells. These data indicate that multiple signaling pathways are involved in presynaptic development and that these cues can act independently to regulate synapse assembly and function. In vitro studies demonstrate that synapse number remained similar in both β-catenin knockout cells and scribble knockdown cells. It would be interesting to see whether disrupting scribble in vivo affects synapse number. Indeed, in β-catenin conditional knockout mice, there was a significant increase in synapse number, which is potentially due to compensatory mechanisms (Bamji *et al.*, 2003).

Because disruption of intercellular cadherin interactions also results in SV mislocalization (Togashi *et al.*, 2002), it is likely that cadherin, β-catenin, and scribble act in concert to regulate SV localization. How does scribble localize SVs? There are at least two broad possible answers: 1) scribble binds directly to SVs, which in turn "traps" SVs at synapses, or 2) scribble acts as a scaffold to recruit other proteins to modulate SV localization.

The role of cadherin, β-catenin and scribble in regulating SV localization has been demonstrated in both invertebrate and vertebrate systems. Disruption of *Drosophila* N-cadherin (*D*N-cadherin) results in an aberrant overaccumulation of SVs at synapses formed between photoreceptor cells and their target interneurons (Iwai *et al.*, 2002). Similarly, in *Drosophila* scribble mutants, there is an overaccumulation of SVs at the NMJ (Roche *et al.*, 2002). In contrast, in vertebrate hippocampal cultures, disruption of intercellular N-cadherin contacts results in a mislocalization of SVs that are more diffusely distributed along the axon (Togashi *et al.*, 2002). Moreover, ablation of β-catenin in conditional knockout mice results in a decreased number of vesicles associated with synapses, corresponding to a more diffuse pattern of SV localization in cultured hippocampal neurons (Bamji *et al.*, 2003). In N-cadherin knockout embryonic stem cell–derived neurons, there is a clear presynaptic defect in the availability of vesicles for exocytosis and a coincident alteration in short-term plasticity properties (Jungling *et al.*, 2006). A detailed quantification of the number of SVs per synapse is lacking in this study; however, the gross similarity between wild-type and mutant mice may be due to the expression of additional classic cadherins at the hippocampal synapse. It is currently unknown whether there is a disparity between vertebrate and invertebrate systems or whether differences in SV phenotypes arise from differences in synapse type.

It has previously been shown that the number of SVs at presynaptic compartments can contribute to the regulation of synaptic function (Cabin *et al.*, 2002; Bamji *et al.*, 2003) and that this can be modulated by homeostatic mechanisms in response to changes in synaptic activity (Murthy *et al.*, 2001; Thiagarajan *et al.*, 2005). Synaptic activity has also been shown to modulate synaptic adhesion. Indeed, alterations in activity can modulate both N-cadherin expression levels (Bozdagi *et al.*, 2000) and levels of N-cadherin dimerization (Tanaka *et al.*, 2000). These findings suggest that synaptic activity may regulate SV localization through modulation of cadherin–β-catenin adhesion complexes. Understanding the molecular mechanisms underlying SV recruitment and localization is therefore important not only for our understanding of the development and maintenance of synapses, but also for our understanding of how these signaling pathways could be used by neurons to modulate synaptic properties. Our data demonstrate a critical role for scribble in localizing SVs and provide an important link between scribble and the cadherin–β-catenin complex.

ACKNOWLEDGMENTS

This work was supported by grants from the National Health and Medical Research Council of Australia (P.O.H.), Association for International Cancer Research UK (P.O.H.), Canadian Institutes of Health Research Grant MOP-81158 (S.X.B.), the Pacific Alzheimer's Research Foundation Grant OP06-09 (S.X.B.), and the American Alzheimer's Association Grant NIRG-07-58917 (S.X.B.).

REFERENCES

Ahmari, S. E., Buchanan, J., and Smith, S. J. (2000). Assembly of presynaptic active zones from cytoplasmic transport packets. Nat. Neurosci. *3*, 445–451.

Audebert, S., *et al.* (2004). Mammalian Scribble forms a tight complex with the betaPIX exchange factor. Curr. Biol. *14*, 987–995.

Bamji, S. X., Rico, B., Kimes, N., and Reichardt, L. F. (2006). BDNF mobilizes synaptic vesicles and enhances synapse formation by disrupting cadherin-beta-catenin interactions. J. Cell Biol. *174*, 289–299.

Bamji, S. X., Shimazu, K., Kimes, N., Huelsken, J., Birchmeier, W., Lu, B., and Reichardt, L. F. (2003). Role of beta-catenin in synaptic vesicle localization and presynaptic assembly. Neuron *40*, 719–731.

Bozdagi, O., Shan, W., Tanaka, H., Benson, D. L., and Huntley, G. W. (2000). Increasing numbers of synaptic puncta during late-phase LTP: N-cadherin is synthesized, recruited to synaptic sites, and required for potentiation. Neuron *28*, 245–259.

Cabin, D. E., *et al.* (2002). Synaptic vesicle depletion correlates with attenuated synaptic responses to prolonged repetitive stimulation in mice lacking alpha-synuclein. J. Neurosci. *22*, 8797–8807.

Daniels, D. L., Eklof Spink, K., and Weis, W. I. (2001). Beta-catenin: molecular plasticity and drug design. Trends Biochem. Sci. *26*, 672–678.

Darcy, K. J., Staras, K., Collinson, L. M., and Goda, Y. (2006a). Constitutive sharing of recycling synaptic vesicles between presynaptic boutons. Nat. Neurosci. *9*, 315–321.

Darcy, K. J., Staras, K., Collinson, L. M., and Goda, Y. (2006b). An ultrastructural readout of fluorescence recovery after photobleaching using correlative light and electron microscopy. Nat. Protoc. *1*, 988–994.

Dow, L. E., Kauffman, J. S., Caddy, J., Zarbalis, K., Peterson, A. S., Jane, S. M., Russell, S. M., and Humbert, P. O. (2007). The tumour-suppressor Scribble dictates cell polarity during directed epithelial migration: regulation of Rho GTPase recruitment to the leading edge. Oncogene *26*, 2272–2282.

Dow, L. E., Brumby, A. M., Muratore, R., Coombe, M. L., Sedelies, K. A., Trapani, J. A., Russell, S. M., Richardson, H. E., and Humbert, P. O. (2003). hScrib is a functional homologue of the *Drosophila* tumour suppressor Scribble. Oncogene *22*, 9225–9230.

Gerrow, K., Romorini, S., Nabi, S. M., Colicos, M. A., Sala, C., and El-Husseini, A. (2006). A preformed complex of postsynaptic proteins is involved in excitatory synapse development. Neuron *49*, 547–562.

Ivanov, D. B., Philippova, M. P., and Tkachuk, V. A. (2001). Structure and functions of classical cadherins. Biochemistry *66*, 1174–1186.

Iwai, Y., Hirota, Y., Ozaki, K., Okano, H., Takeichi, M., and Uemura, T. (2002). DN-cadherin is required for spatial arrangement of nerve terminals and ultrastructural organization of synapses. Mol. Cell Neurosci. *19*, 375–388.

Jungling, K., Eulenburg, V., Moore, R., Kemler, R., Lessmann, V., and Gottmann, K. (2006). N-cadherin transsynaptically regulates short-term plasticity at glutamatergic synapses in embryonic stem cell-derived neurons. J. Neurosci. *26*, 6968–6978.

Kalla, S., Stern, M., Basu, J., Varoqueaux, F., Reim, K., Rosenmund, C., Ziv, N. E., and Brose, N. (2006). Molecular dynamics of a presynaptic active zone protein studied in Munc13-1-enhanced yellow fluorescent protein knock-in mutant mice. J. Neurosci. *26*, 13054–13066.

Kamei, Y., Kito, K., Takeuchi, T., Imai, Y., Murase, R., Ueda, N., Kobayashi, N., and Abe, Y. (2007). Human scribble accumulates in colorectal neoplasia in association with an altered distribution of beta-catenin. Hum. Pathol. *38*, 1273–1281.

Krueger, S. R., Kolar, A., and Fitzsimonds, R. M. (2003). The presynaptic release apparatus is functional in the absence of dendritic contact and highly mobile within isolated axons. Neuron *40*, 945–957.

Ludford-Menting, M. J., *et al.* (2005). A network of PDZ-containing proteins regulates T cell polarity and morphology during migration and immunological synapse formation. Immunity *22*, 737–748.

Mathew, D., Gramates, L. S., Packard, M., Thomas, U., Bilder, D., Perrimon, N., Gorczyca, M., and Budnik, V. (2002). Recruitment of scribble to the synaptic scaffolding complex requires GUK-holder, a novel DLG binding protein. Curr. Biol. *12*, 531–539.

Murthy, V. N., Schikorski, T., Stevens, C. F., and Zhu, Y. (2001). Inactivity produces increases in neurotransmitter release and synapse size. Neuron *32*, 673–682.

Navarro, C., *et al.* (2005). Junctional recruitment of mammalian Scribble relies on E-cadherin engagement. Oncogene *24*, 4330–4339.

Nguyen, M. M., Rivera, C., and Griep, A. E. (2005). Localization of PDZ domain containing proteins Discs Large-1 and Scribble in the mouse eye. Mol. Vis. *11*, 1183–1199.

Perego, C., Vanoni, C., Massari, S., Longhi, R., and Pietrini, G. (2000). Mammalian LIN-7 PDZ proteins associate with beta-catenin at the cell-cell junctions of epithelia and neurons. EMBO J. *19*, 3978–3989.

Roche, J. P., Packard, M. C., Moeckel-Cole, S., and Budnik, V. (2002). Regulation of synaptic plasticity and synaptic vesicle dynamics by the PDZ protein Scribble. J. Neurosci. *22*, 6471–6479.

Rossner, M., and Yamada, K. M. (2004). What's in a picture? The temptation of image manipulation. J. Cell Biol. *166*, 11–15.

Sankaranarayanan, S., and Ryan, T. A. (2000). Real-time measurements of vesicle-SNARE recycling in synapses of the central nervous system. Nat. Cell Biol. *2*, 197–204.

Santoni, M. J., Pontarotti, P., Birnbaum, D., and Borg, J. P. (2002). The LAP family: a phylogenetic point of view. Trends Genet. *18*, 494–497.

Schweizer, F. E., and Ryan, T. A. (2006). The synaptic vesicle: cycle of exocytosis and endocytosis. Curr. Opin. Neurobiol. *16*, 298–304.

Staras, K. (2007). Share and share alike: trading of presynaptic elements between central synapses. Trends Neurosci. *30*, 292–298.

Su, L. K., Vogelstein, B., and Kinzler, K. W. (1993). Association of the APC tumor suppressor protein with catenins. Science *262*, 1734–1737.

Sudhof, T. C. (2004). The synaptic vesicle cycle. Annu. Rev. Neurosci. *27*, 509–547.

Takizawa, S., *et al.* (2006). Human scribble, a novel tumor suppressor identified as a target of high-risk HPV E6 for ubiquitin-mediated degradation, interacts with adenomatous polyposis coli. Genes Cells *11*, 453–464.

Tanaka, H., Shan, W., Phillips, G. R., Arndt, K., Bozdagi, O., Shapiro, L., Huntley, G. W., Benson, D. L., and Colman, D. R. (2000). Molecular modification of N-cadherin in response to synaptic activity. Neuron *25*, 93–107.

Taschenberger, H., Leao, R. M., Rowland, K. C., Spirou, G. A., von Gersdorff, H. (2002). Optimizing synaptic architecture and efficiency for high-frequency transmission. Neuron *36*, 1127–1143.

Thiagarajan, T. C., Lindskog, M., and Tsien, R. W. (2005). Adaptation to synaptic inactivity in hippocampal neurons. Neuron *47*, 725–737.

Togashi, H., Abe, K., Mizoguchi, A., Takaoka, K., Chisaka, O., and Takeichi, M. (2002). Cadherin regulates dendritic spine morphogenesis. Neuron *35*, 77–89.

Tsuriel, S., Geva, R., Zamorano, P., Dresbach, T., Boeckers, T., Gundelfinger, E. D., Garner, C. C., and Ziv, N. E. (2006). Local sharing as a predominant determinant of synaptic matrix molecular dynamics. PLoS Biol. *4*, e271.

Xie, C., Markesbery, W. R., and Lovell, M. A. (2000). Survival of hippocampal and cortical neurons in a mixture of MEM+ and B27-supplemented neurobasal medium. Free Radic Biol. Med. *28*, 665–672.

Yamanaka, T., and Ohno, S. (2008). Role of Lgl/Dlg/Scribble in the regulation of epithelial junction, polarity and growth. Front. Biosci. *13*, 6693–6707.

Zhai, R. G., Vardinon-Friedman, H., Cases-Langhoff, C., Becker, B., Gundelfinger, E. D., Ziv, N. E., and Garner, C. C. (2001). Assembling the presynaptic active zone: a characterization of an active one precursor vesicle. Neuron *29*, 131–143.

Ziv, N. E., and Garner, C. C. (2004). Cellular and molecular mechanisms of presynaptic assembly. Nat. Rev. Neurosci. *5*, 385–399.